

Squark and Gluino Production with Jets

T. Plehn,¹ D. Rainwater,² and P. Skands³

¹*Heisenberg Fellow, Max Planck Institute for Physics, Munich, Germany*

²*Marshak Fellow, Dept. of Physics and Astronomy, University of Rochester, Rochester, USA*

³*Theoretical Physics Dept., Fermi National Accelerator Laboratory, Batavia, USA*

(Dated: October 6, 2018)

We present cross section predictions for squark and gluino production at the LHC, in association with up to two additional hard jets. These cross sections can be very large in comparison to the inclusive Born rates. Because hadron collider experiments utilize hard jets in the reconstruction of cascade decays or as a way to separate squark and gluino production, the understanding of these processes is crucial. We show to what degree hard jet radiation can be described by shower algorithms and point out how tuning these showers, for example to top quark pair production, could help reduce theoretical uncertainties for new physics searches at the LHC.

In the Standard Model (SM), the mechanism of the observed electroweak symmetry breaking is widely believed to involve a Higgs boson. This fundamental scalar poses a theoretical problem: the stability of its mass after the inclusion of radiative corrections. A possible solution is TeV-scale supersymmetry. The minimal supersymmetric extension of the Standard Model (MSSM) simultaneously solves several problems in high energy physics and cosmology: gauge coupling unification; radiative electroweak symmetry breaking [1]; and a stable weakly-interacting dark matter candidate [2].

With the Tevatron in operation and the LHC only a few years distant, the TeV scale is rapidly coming within reach. Squark and gluino production cross sections approach $\mathcal{O}(\text{pb})$ at the Tevatron and $\mathcal{O}(\text{nb})$ at the LHC, for masses around the present Tevatron exclusion limits of up to 400 GeV.

MSSM searches and jets: The main difference between R-parity-conserving MSSM signals and SM QCD backgrounds at a hadron collider comes from the stable lightest supersymmetric particle, an end product of all superpartner decays, which escapes the detector unobserved. Requiring a large amount of missing transverse energy is thus the first ingredient to enhance the signal. The QCD-strength production channels for squarks and gluinos are $pp \rightarrow \tilde{g}\tilde{g}, \tilde{q}\tilde{q}^*, \tilde{q}\tilde{q}, \tilde{q}\tilde{g}$ [3, 4]. To a good approximation, the light-flavor MSSM squarks are mass degenerate, while the lighter of the two top squarks is often the lightest strongly-interacting MSSM particle. Searching for squarks and gluinos in an inclusive analysis the signature is jets plus \cancel{E}_T , possibly plus leptons. The shortest cascade of two-particle decays is $\tilde{g} \rightarrow \tilde{q}\tilde{q}$ and $\tilde{q} \rightarrow q\tilde{\chi}_1^0$, where the lightest neutralino $\tilde{\chi}_1^0$ is stable. Such an inclusive search is well-suited to find MSSM-type deviations from the Standard Model. Because the gluino decay gives one more hard jet in the final state, an event's jet multiplicity provides discrimination between the relative rates of squarks and gluinos.

We can also make use of longer decay chains, *e.g.* of the classic type $\tilde{g} \rightarrow \tilde{q}\tilde{q} \rightarrow \tilde{\chi}_2^0 q\tilde{q} \rightarrow \tilde{\ell}\tilde{\ell}q\tilde{q} \rightarrow \tilde{\chi}_1^0 \ell\ell q\tilde{q}$ with

five unknown masses. These masses can be extracted from kinematic distributions, *i.e.* thresholds and edges of different momentum combinations [5]. Alternative methods have been developed to improve the mass reconstruction [6] and the associated statistical and systematic errors. These measurements can in turn be used to determine parameters of the TeV-scale MSSM Lagrangian [7].

To make optimal use of the achievable statistical precision, as well as to quantify the errors on extracted model parameters, it is crucial to properly understand the systematic errors in the cascade reconstruction. Obviously, effects such as detector resolution and jet energy scale calibration will have a large impact [8]. In this letter, we focus on another source of (combinatorial) error: the presence of additional, observable hard jets due to SM QCD radiation, with transverse momenta comparable to the typical cuts planned for squark and gluino studies, about $p_T > 50 - 100$ GeV [9, 10]. Extra jets, in particular from the initial state, will introduce noise when reconstructing the cascade kinematics from the observed jet kinematics and when attempting to separate squark- and gluino-enriched samples. This question has a counterpart in the hadronic top analyses at the Tevatron. We know from data that in these analyses additional jet radiation fakes W decay jets in a non-trivial fraction of the events [11]. With generally larger energy scales involved in SUSY processes, one would expect the initial state to

	$\sigma_{\text{tot}}[\text{pb}]$	$\tilde{g}\tilde{g}$	$\tilde{u}_L\tilde{g}$	$\tilde{u}_L\tilde{u}_L^*$	$\tilde{u}_L\tilde{u}_L$	$T\bar{T}$
$p_{T,j} > 100 \text{ GeV}$	σ_{0j}	4.83	5.65	0.286	0.502	1.30
	σ_{1j}	2.89	2.74	0.136	0.145	0.73
	σ_{2j}	1.09	0.85	0.049	0.039	0.26
$p_{T,j} > 50 \text{ GeV}$	σ_{0j}	4.83	5.65	0.286	0.502	1.30
	σ_{1j}	5.90	5.37	0.283	0.285	1.50
	σ_{2j}	4.17	3.18	0.179	0.117	1.21

Table I: Cross sections for the production of a toy-model 600 GeV top quark, squarks and gluinos at the LHC at the benchmark point SPS1a. We show fixed-order matrix element results with 0,1,2 additional hard jets, and with two different $p_{T,j}^{\text{min}}$ values and $|y_j| < 5$ and $R_{jj} > 0.4$.

be more active, hence potentially more dangerous.

Hard jets from matrix elements: To study the production of hard jets with squarks and gluinos at the LHC, we first present the results of a fixed-order approach. We use the new supersymmetric version [12, 13] of the event generator MadEvent [14] to calculate tree-level rates for $pp \rightarrow \tilde{g}\tilde{g}, \tilde{q}\tilde{q}^*, \tilde{q}\tilde{q}, \tilde{q}\tilde{g}$, including the emission of one and two additional jets. To avoid regions sensitive to the soft and collinear singularities of initial- and final-state radiation we limit ourselves to $p_{T,j} > 50$ GeV (and in some cases $p_{T,j} > 100$ GeV), for which we expect fixed-order perturbation theory to be reliable at the LHC.

In Table I we show inclusive production cross section estimates for squarks and gluinos plus zero to two hard jets, for the parameter point SPS1a, where $m_{\tilde{g}} = 608$ GeV and $m_{\tilde{u}_L} = 567$ GeV [15]. The factorization scale is set to the average final state mass, as is the renormalization scale for the heavy pair. The renormalization scale for additional jet radiation is $p_{T,j}$, the standard choice in shower Monte Carlos [16]. We see that for jets with $p_T > 100$ GeV the perturbative expansion is stable, but the relative suppression is closer to $1/2 \cdots 1/3$ than to α_s/π . If we allow semi-hard jets down to 50 GeV the fixed-order perturbative expansion approaches its limit. We emphasize that it is not a problem for the one-jet rate to be slightly larger than the all-inclusive rate at leading order, as long as it is in the range of the NLO inclusive cross section [4]. To check that this behavior is quantitatively universal for heavy QCD production we also show the rates for a heavy toy-quark T (effectively a 600 GeV top), and we indeed see the same pattern.

The case of gluino pair production exemplifies that gluon radiation (mostly from the initial state) is indeed the dominant source of extra jets: allowing just initial- and final-state gluons with $p_{T,j} > 50$ GeV, the $\tilde{g}\tilde{g}$ case in Table I becomes $\sigma_{0,1,2j} = (4.63, 3.90, 2.03)$ pb. In addition, jet radiation probes new initial states through crossing of quarks and gluons from the final state to the initial state: *e.g.* purely quark-initiated processes like $qq \rightarrow \tilde{q}\tilde{q}$ receive large corrections from qg scattering. These crossed channels include intermediate states of the kind $qg \rightarrow \tilde{q}\tilde{g} \rightarrow \tilde{q}\tilde{q}\tilde{g}$. Usually these intermediate states are subtracted in the narrow-width approximation to avoid double counting between NLO $\tilde{q}\tilde{q}$ and $\tilde{g}\tilde{g}$ production [4]. Here, we explicitly remove all on-shell intermediate gluinos from $\tilde{g}\tilde{u}_L$ production. For the $\tilde{u}_L\tilde{u}_L^{(*)}$ channel we simply decrease the gluino mass to 558 GeV to avoid intermediate on-shell gluinos.

Jets from parton showers: To compare to experimental observables, multiple soft emission and hadronization effects can be important – aspects which go beyond the scope of a fixed-order calculation. For bremsstrahlung emission, logarithms $\alpha_s^N \log^{2N}(Q_{\text{soft}}^2/Q_{\text{hard}}^2)$ appear to all orders in perturbation theory, while the correc-

tions associated with hadronization are inherently non-perturbative, $\alpha_s \rightarrow 1$. Exploiting collinear factorization in QCD and assuming universality of hadronization, both types of corrections may be included, at least approximately. This is the basis of multi-purpose event generators like HERWIG, PYTHIA, or SHERPA. Starting from a given set of final state partons, a sequence of initial- and final-state QCD branchings are generated, resumming the leading logarithms mentioned above. The emissions are ordered, *e.g.* in the parton virtuality Q or in $p_{T,j}$, and the description is matched to hadronization models at a fixed low scale, ~ 1 GeV.

Especially for hard radiation, large differences may exist between different shower algorithms. To quantify, we use PYTHIA [17] with two qualitatively different showers: one Q^2 -ordered [18], and the other p_T -ordered [19]. Note that, due to the large final state squark and gluino masses, we explore mainly the properties of the initial-state showers. The crucial parameter here is the starting scale of the shower, which sets an upper limit to the phase space over which jets can be radiated. For initial-state radiation, this starting scale is nominally identical to the factorization scale, where the parton densities are convoluted with the matrix elements. In PYTHIA, this scale is normally the transverse mass $\mu_F = \sqrt{p_T^2 + \hat{m}^2}$, with \hat{m} the average mass of the final state SUSY particles, and p_T their relative transverse momentum.

For a p_T -ordered shower, this μ_F can be used directly as the maximum $p_{T,j}$. We refer to this choice as the p_T -ordered ‘wimpy shower’. We also investigate the consequences of allowing the parton shower to populate the full phase space, with the maximum $p_{T,j} = \sqrt{s}/2$, regardless of μ_F . This choice we refer to as the p_T -ordered ‘power shower’. Though strictly-speaking in conflict with the factorization assumption, this choice has interesting phenomenological consequences, as we shall see.

The case of a Q^2 -ordered shower is not so simple. The starting scale here is $Q_{\text{max}}^2 = \min(C\mu_F^2, s)$, where $C \geq 1$ parameterizes the translation from p_T^2 to Q^2 . We refer to $C = 1$ as the Q^2 -ordered wimpy shower, $C = 4$ as Tune A [20] (designed to match Tevatron data), and $C \rightarrow \infty$ as power shower — with the same caveat concerning factorization as for the p_T -ordered version.

Numerical Comparison: We now turn to a comparison of the three processes $t\bar{t}$ +jets, $\tilde{g}\tilde{g}$ +jets, and $\tilde{u}_L\tilde{u}_L$ +jets, at the LHC. Here, $t\bar{t}$ represents a process with a small ratio μ_F/\sqrt{s} , while the SUSY processes involve much larger masses and hence larger factorization scales. The difference between $\tilde{g}\tilde{g}$ and $\tilde{u}_L\tilde{u}_L$ is the sea- v. valence-dominated initial state.

Jets in the parton shower final states were clustered using a cone algorithm with $\Delta R = 0.4$, *i.e.* similar to the ME cut $R_{j,j} > 0.4$. By looking at $p_{T,j}/p_{T,\text{ME}}$ in generated dijet samples, we checked explicitly that out-of-cone corrections are too small to affect our study significantly.

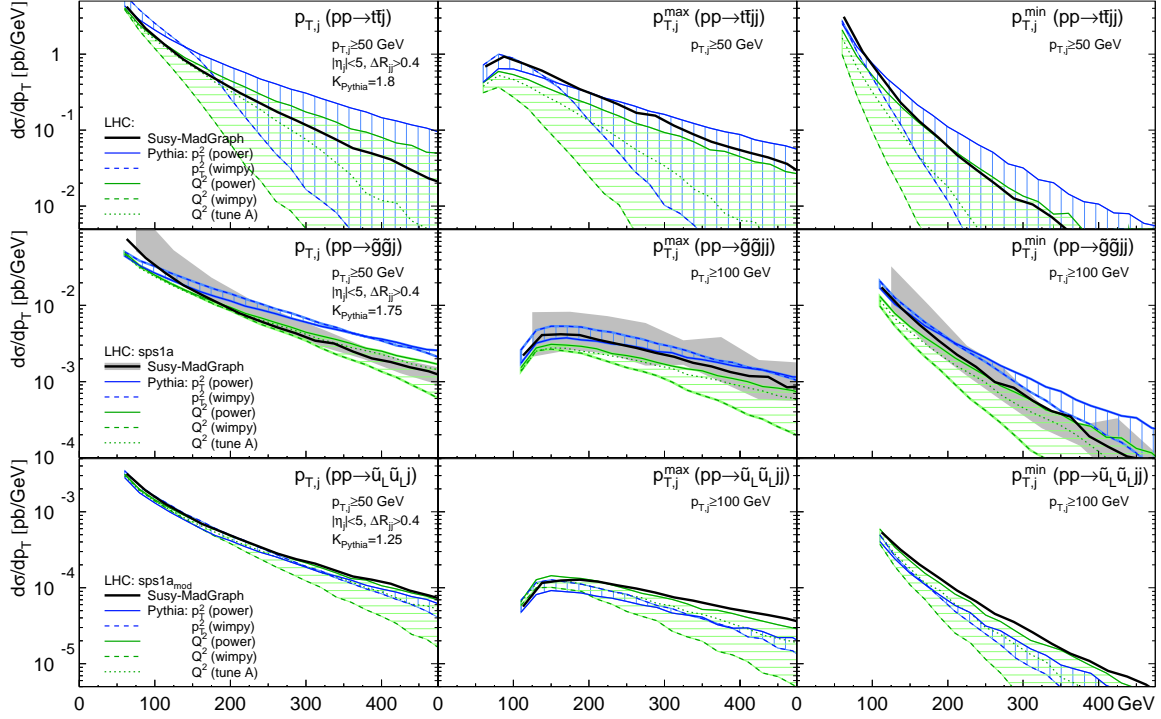


Figure 1: $p_{T,j}$ spectra for $t\bar{t}$, $\tilde{g}\tilde{g}$ and $\tilde{u}_L\tilde{u}_L$ production in association with 1 and 2 hard jets. NLO K-factors [4] are applied to the PYTHIA results to avoid a normalization mismatch in the one-jet case. The mass spectrum is given by SPS1a, except for $\tilde{u}_L\tilde{u}_L$ where we reduced the gluino mass, as in Tab. I. At high p_T (of order the factorization scale and above), the matrix elements are, by definition, the most reliable while the parton showers can be seen to be associated with large uncertainties, whereas the opposite is the case at low p_T . The shaded region in the middle row is the theoretical uncertainty on the matrix element prediction. See text for details.

In Fig. 1 we show results for the $p_{T,j}$ spectra, using CTEQ5L parton distribution functions [21]. We use the heavy particle mass as the central value for the factorization scale. For renormalization scale, we apply one factor of α_s using $Q^2 = m_T^2$ for each final-state particle. The shaded band in the middle row highlights the theoretical uncertainty by plotting the extremal values of four factorization and renormalization scale choices: varying μ_R down to the minimum p_T of the jets, and varying μ_F down to the minimum p_T of the jets and up to $\sqrt{s}/2$.

Consider first $t\bar{t}+1\text{jet}$ (upper left): as a general feature, the power showers exhibit a harder high- p_T spectrum than the matrix element. In contrast, note the cataclysmic drop of the wimpy showers above $p_{T,j} \sim m_t \sim \mu_F$, with the Q^2 -ordered wimpy showers everywhere softer than the matrix element. Finally, Tune A is indistinguishable from the matrix element for $p_{T,j} < 250$ GeV, this region being similar to the phase space accessible at the Tevatron. All the calculations agree fairly well down to $p_{T,j} \sim 50$ GeV, a value sufficiently below the factorization scale for the parton showers to be reliable, but still large enough for stable fixed-order predictions. The crossover at ~ 150 GeV between the two p_T -ordered showers illustrates the effect of changing μ_R from $p_T/2$ in the wimpy shower to $3p_T$ in the power shower. The Q^2 -ordered showers all use $\mu_R = p_{T,j}$.

For the two-jet distributions, note that the collinear approximation is only rigorously correct in the limit that each successive jet is much softer than the preceding one, hence the two-jet shower predictions are associated with even larger uncertainties. Nevertheless, the power showers deviate from the matrix element by less than a factor two over most of the $p_{T,j}$ range. Although remaining differences could undoubtedly be cured by slight shower parameter modifications, we note that obtaining simultaneous agreement of the one- and two-jet rates is likely to require more sophisticated matching techniques [24–27].

The parton shower predictions for the SUSY processes exhibit significantly less variation, as shown in the lower rows of Fig. 1. Owing to much larger factorization scales the presence or absence of a cutoff in the parton shower evolution at μ_F does not lead to very large differences for the $p_{T,j}$ regions we consider. In this way, the kinematic regime of squark and gluino production at the LHC is more similar to *e.g.* $t\bar{t}$ production at the Tevatron than at the LHC. Considering first $\tilde{g}\tilde{g}+1\text{jet}$, we observe that the matrix element rate begins to diverge around $p_{T,j} \sim 100$ GeV, due to large logarithms, $\log^2 m_{\tilde{g}}^2/p_{T,j}^2$. For Z , light Higgs, or even $t\bar{t}$ production this breakdown scale is much smaller, of order the minimum $p_{T,j}$ observable at the LHC [23]. The case of heavy particle production, such as gluinos and squarks, is different: for jets softer

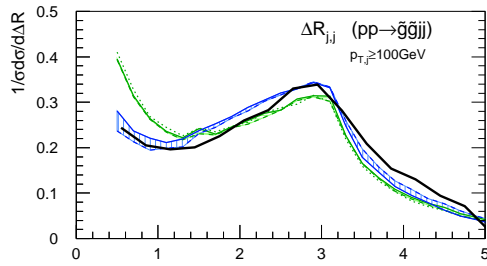


Figure 2: The ΔR_{jj} distribution for $\tilde{g}\tilde{g}jj$ production as predicted by the hard matrix element and the parton showers.

than $p_T \sim 100$ GeV we would be well-advised to include resummation effects.

At large values of $p_{T,j}$, a pattern similar to the tops arises: the one-jet radiation is very well described by Tune A. For two-jet radiation, the Q^2 -ordered showers generally fall below the matrix element, while the p_T -ordered ones overshoot. We also studied $\tilde{u}_L\tilde{u}_L^*$ and $\tilde{u}_L\tilde{g}$ production and found that they exhibit essentially the same behavior as gluino-pair production.

For the last process in Fig. 1, $\tilde{u}_L\tilde{u}_L$ production, the matrix element divergence at low p_T appears to be much milder than for the $\tilde{g}\tilde{g}$ case. We interpret this as a consequence of the less radiating, valence-dominated initial state. For the high- p_T tail, the power showers are again in fairly good agreement with the matrix element, though with a much smaller difference between p_T - and Q^2 -ordered showers than above.

Lastly, we compare the ΔR_{jj} distributions for gluino pairs plus two jets in Fig. 2. The results are not drastically different. The difference between the two different shower models at low ΔR is interesting, however. It should probably not be interpreted as the onset of a collinear singularity. In that case, one would expect the showers to agree with each other, but not with the matrix elements. Moreover, from the results presented in Fig. 1 it is clear that with a jet cut of 100 GeV we are nowhere near the collinear region. In fact, the cutoff itself may furnish part of the reason; the region where both jets are close to the cutoff is, by definition, not strongly ordered, and would hence be expected to be problematic for shower descriptions. We plan to return to this in a future study.

Summary: Using SUSY-MadEvent we show that matrix-element-based QCD calculations predict a large number of hard jets associated with squark and gluino production at the LHC. This effect should be taken into account in studies of the separation of squark and gluino event samples, and for cascade decay reconstruction. We compared in detail the matrix element approach and the results from p_T -ordered and Q^2 -ordered showers, implemented in PYTHIA 6.3.

For the radiation of one extra jet in SUSY heavy colored pair production processes, conventional parton showers with a phase space cutoff at the factorization

scale give a reasonable approximation up to $p_{T,j} \sim \mu_F/2$, above which they rapidly break down. This is similar to what has been observed before for Drell-Yan [25, 28, 29] (and Higgs) production. A significant improvement can be obtained by removing the explicit phase space cut, allowing the shower to populate all of phase space. However, this tends to yield somewhat harder radiation spectra than produced by the matrix elements, again akin to what has been shown for hadroproduction of colorless resonances [29].

For fairly soft jets, we see that in the production of high-mass gluinos the breakdown of fixed-order perturbation theory caused by logarithmic corrections can occur already at jet transverse momenta of as high as 100 GeV.

We would like to thank Kaoru Hagiwara and Tim Stelzer for their great help creating SUSY-MadEvent; Torbjorn Sjöstrand for enlightening discussions and comments on the manuscript; and finally the Madison Pheno group, the DESY and KEK theory groups, and the Aspen Center for Physics for their generous hospitality. This research was supported in part by the U.S. Department of Energy under grant Nos. DE-FG02-91ER40685 and DE-AC02-76CH03000.

-
- [1] For reviews of SUSY, see *e.g.* : I. J. R. Aitchison, hep-ph/0505105; S. P. Martin, hep-ph/9709356.
 - [2] J. R. Ellis, J. S. Hagelin, D. V. Nanopoulos, K. A. Olive and M. Srednicki, Nucl. Phys. B **238**, 453 (1984); H. Goldberg, Phys. Rev. Lett. **50**, 1419 (1983); for a recent review see *e.g.* : G. Bertone, D. Hooper and J. Silk, Phys. Rept. **405**, 279 (2005).
 - [3] S. Dawson, E. Eichten and C. Quigg, Phys. Rev. D **31**, 1581 (1985).
 - [4] W. Beenakker, R. Höpker, M. Spira and P. M. Zerwas, Nucl. Phys. B **492**, 51 (1997); W. Beenakker, M. Krämer, T. Plehn, M. Spira and P. M. Zerwas, Nucl. Phys. B **515**, 3 (1998); W. Beenakker, M. Klasen, M. Krämer, T. Plehn, M. Spira and P. M. Zerwas, Phys. Rev. Lett. **83**, 3780 (1999).
 - [5] H. Bachacou, I. Hinchliffe and F. E. Paige, Phys. Rev. D **62**, 015009 (2000); B. C. Allanach, C. G. Lester, M. A. Parker and B. R. Webber, JHEP **0009**, 004 (2000).
 - [6] K. Kawagoe, M. M. Nojiri and G. Polesello, Phys. Rev. D **71**, 035008 (2005).
 - [7] R. Lafaye, T. Plehn and D. Zerwas, hep-ph/0404282; P. Bechtle, K. Desch and P. Wienemann, hep-ph/0412012.
 - [8] B. K. Gjelsten, D. J. Miller and P. Osland, JHEP **0412**, 003 (2004) and hep-ph/0501033.
 - [9] ATLAS TDR, report CERN/LHCC/1999-15 (1999).
 - [10] CMS TDR, report CERN/LHCC/2006-001 (2006).
 - [11] L. Orr, private communication; R. Demina, private communication.
 - [12] G.-C. Cho, K. Hagiwara, J. Kanzaki, T. Plehn, D. Rainwater and T. Stelzer, in preparation.

- [13] K. Hagiwara, W. Kilian, F. Krauss, T. Ohl, T. Plehn, D. Rainwater J. Reuter and S. Schumann, hep-ph/0512260.
- [14] T. Stelzer, F. Long, Comput. Phys. Commun. **81** (1994) 357; F. Maltoni and T. Stelzer, JHEP **0302**, 027 (2003).
- [15] B. C. Allanach *et al.*, Eur. Phys. J. C **25**, 113 (2002).
- [16] D. Amati, A. Bassetto, M. Ciafaloni, G. Marchesini and G. Veneziano, Nucl. Phys. B **173**, 429 (1980); G. Curci, W. Furmanski and R. Petronzio, Nucl. Phys. B **175**, 27 (1980).
- [17] T. Sjöstrand, P. Eden, C. Friberg, L. Lönnblad, G. Miu, S. Mrenna and E. Norrbin, Comput. Phys. Commun. **135**, 238 (2001) T. Sjöstrand, L. Lönnblad, S. Mrenna and P. Skands, hep-ph/0308153.
- [18] T. Sjöstrand, Phys. Lett. B **157**, 321 (1985); M. Bengtsson, T. Sjöstrand and M. van Zijl, Z. Phys. C **32**, 67 (1986); M. Bengtsson and T. Sjöstrand, Phys. Lett. B **185**, 435 (1987) and Nucl. Phys. B **289**, 810 (1987).
- [19] T. Sjöstrand and P. Z. Skands, Eur. Phys. J. C **39**, 129-154 (2005).
- [20] R.D. Field, hep-ph/0201192 CDF Note 6403; further recent talks available from webpage <http://www.phys.ufl.edu/~rfield/cdf/>
- [21] H. L. Lai *et al.* [CTEQ Collaboration], Eur. Phys. J. C **12**, 375 (2000).
- [22] P. Nason, S. Dawson and R. K. Ellis, Nucl. Phys. B **303**, 607 (1988); M. L. Mangano, P. Nason and G. Ridolfi, Nucl. Phys. B **373**, 295 (1992); W. Beenakker, W. L. van Neerven, R. Meng, G. A. Schuler and J. Smith, Nucl. Phys. B **351**, 507 (1991); R. Bonciani, S. Catani, M. L. Mangano and P. Nason, Nucl. Phys. B **529**, 424 (1998); W. Bernreuther, A. Brandenburg, Z. G. Si and P. Uwer, Nucl. Phys. B **690**, 81 (2004); for a review see *e.g.* : M. Beneke *et al.*, hep-ph/0003033.
- [23] J. C. Collins and D. E. Soper, Nucl. Phys. B **193**, 381 (1981) [Erratum-ibid. B **213**, 545 (1983)]; J. C. Collins and D. E. Soper, Nucl. Phys. B **197**, 446 (1982); J. C. Collins, D. E. Soper and G. Sterman, Nucl. Phys. B **250**, 199 (1985); C. T. H. Davies, B. R. Webber and W. J. Stirling, Nucl. Phys. B **256**, 413 (1985); G. Bozzi, S. Catani, D. de Florian and M. Grazzini, hep-ph/0508068.
- [24] S. Catani, F. Krauss, R. Kuhn and B. R. Webber, JHEP **0111**, 063 (2001); L. Lönnblad, JHEP **0205**, 046 (2002); P. Nason, JHEP **0411**, 040 (2004); Z. Nagy and D. E. Soper, hep-ph/0503053.
- [25] S. Mrenna and P. Richardson, JHEP **0405**, 040 (2004).
- [26] S. Frixione and B. R. Webber, JHEP **0206**, 029 (2002); S. Frixione, P. Nason and B. R. Webber, JHEP **0308**, 007 (2003).
- [27] S. Höche, F. Krauss, A. Schälicke, S. Schumann and J. C. Winter, JHEP **0402**, 056 (2004);
- [28] see *e.g.* : W. T. Giele, T. Matsuura, M. H. Seymour and B. R. Webber, FERMILAB-CONF-90-228-T; M. H. Seymour, Comput. Phys. Commun. **90**, 95 (1995); J. Huston, I. Puljak, T. Sjöstrand and E. Thomé, hep-ph/0401145 (in hep-ph/0403100); F. Krauss, A. Schälicke, S. Schumann and G. Soff, hep-ph/0503280; N. Lavesson and L. Lönnblad, JHEP **0507**, 054 (2005).
- [29] G. Miu and T. Sjöstrand, Phys. Lett. B **449**, 313 (1999).